Modulated optical sieve for sorting of polydisperse microparticles

I. Ricárdez-Vargas, P. Rodríguez-Montero, and R. Ramos-García[a)]
Instituto Nacional de Astrofísica, Óptica y Electrónica, Apdo. Postal 51/216, 72000 Puebla, Mexico

K. Volke-Sepúlveda[a)]
Instituto de Física, UNAM, Apdo. Postal 20-364, 01000 Mexico Distrito Federal, Mexico

(Received 31 August 2005; accepted 2 February 2006; published online 23 March 2006)

We present an all-optical technique that permits sorting within a polydisperse sample of microparticles in the absence of any microfluidic flow. We can sort colloidal samples based on their size and their refractive index. We show experimental and theoretical data for this method. It is based on the specific response of different microparticles to an interference pattern of fringes vibrating with an asymmetric time modulation. The size selectivity arises from the spatial fringe periodicity whereas selection based on refractive index is controlled by the beam power. © *2006 American Institute of Physics*. [DOI: 10.1063/1.2183357]

The development of efficient techniques for separating and sorting ensembles of microparticles, such as colloids, living cells, and macromolecules is a major goal in multidisciplinary research. The proposal of size separation of colloidal particles using radiation pressure forces dates back to 1970.[1] A renewed and increasing interest has developed in this area in the last few years due to a large number of applications for this noninvasive method, and the new possibilities of creating large reconfigurable extended patterns of light, which offer the prospect of high throughput for this technique. There are sorting methods using both optical and dielectrophoretic techniques.[2,3] In the optical domain, sorting has primarily relied upon the interaction of hydrodynamic Stokes drag with forces from static single optical beam, for example, optical chromatography[4] or stationary extended light patterns (often termed periodic landscapes of light).[5,6] However, it would be advantageous to explore and develop techniques that dispense light with the need for precise microfluidic flow, which would simplify this technology and potentially make it more widely applicable.

The use of periodic potential landscapes in two and three dimensions is the basis for the operation of recently developed microfluidic fractionation systems,[5,6] which can reach efficiencies up to the 100%.[5] Nevertheless, the effective separation of increasingly complex mixtures may result a complicated issue in practice, since it may require considerably complicated tandem systems.[7] On the other hand, one-dimensional lattices or interference fringes have been proposed to sort particles in the absence of microfluidic flow,[8,9] but to the best of our knowledge the effectiveness of these techniques has not been demonstrated yet.

In this letter, we demonstrate an optical fractionation system that requires no microfluidic flow but rather implements an asymmetric time-modulated light pattern achieving high throughput and efficiency that compares with the best currently available, in addition to be able to easily sort mixtures with more than two components. It consists of an interference pattern of fringes vibrating with a sawtooth time modulation, which removes particles of a given size or refractive index from a polydisperse mixture.

[a)]Authors to whom correspondence should be addressed; electronic mail: rgarcia@inaoep.mx, R.R.-G. and karen@fisica.unam.mx K.V.-S.

In contrast to previous work,[8,9] we base our theoretical study on the Mie regime approach. We use a ray tracing model analogous to those described in detail in Refs. 10 and 11 with the intensity distribution adapted to our particular case. The basic equation to obtain the lateral force exerted by a light beam on a dielectric sphere of radius R_0, located at the point (x_0,y_0) of a given transverse plane (z=constant), can be expressed as

$$F(x_0,y_0)=\frac{n_m R_0^2}{2c}\int_0^{\pi/2}\int_0^{2\pi}\left[T^2\left(\frac{\sin 2(\theta_t-\theta)-R\sin 2\theta}{1+R^2+2R\cos 2\theta_t}\right)+R\sin 2\theta\right]\times I(x,y)\sin 2\theta\cos\varphi d\varphi d\theta. \quad (1)$$

The integration is carried out over the illuminated hemisphere of the particle; θ and φ are the polar and azimuthal angles, respectively, in spherical coordinates. In this case, θ coincides with the incidence angle at each point on the sphere's surface and the transmitted angle is denoted by θ_t. R and T represent the reflectance and transmittance coefficients averaged over the two transverse polarization directions at each point[10,11] and n_m is the refractive index of the surrounding medium. The coordinates of each point at the particle's surface, (R_0,φ,θ), and the position of the particle's center with respect to the beam axis, (x_0, y_0), are related by means of $x=x_0+R_0\cos\varphi\sin\theta$, $y=y_0+R_0\sin\varphi\sin\theta$, (for calculations we set $y_0=0$). The incident field is assumed to be Gaussian with a beam waist of $w_0=150$ μm (which is of the order of our experimental value), modulated in the x direction by an interference pattern with spatial period L. The intensity distribution in the focal plane ($z=0$) is given by

$$I(x,y;t)=\frac{4P_0}{\pi w_0^2}\cos^2\left(\frac{\pi x}{L}+\frac{\phi(t)}{2}\right)\exp\left(\frac{-2\rho^2}{w_0^2}\right), \quad (2)$$

where P_0 is the incident power, $\rho^2=x^2+y^2$, and in our case we have a time modulation function of the form $\phi(t)=\phi_0 ft$; $t\in[0,1/f)$, satisfying the periodicity condition $\phi(t+n/f)=\phi(t)$, $(n=0,1,2,\ldots)$. ϕ_0 and f are the maximum phase shift of the oscillation and the vibration frequency, respectively.

In order to elucidate the size selection mechanism, Fig. 1 illustrates some theoretical results for the optical force as a

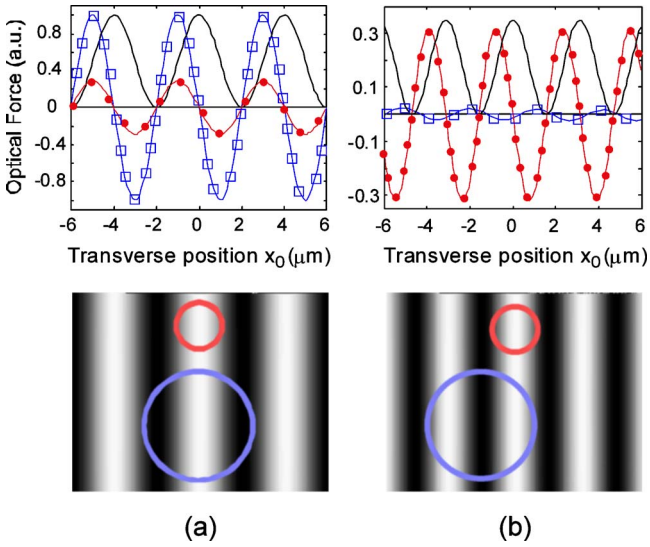

FIG. 1. (Color online) Top row: Optical force vs transverse position (in microns) for spheres with diameters $D_1=2.0$ μm and $D_2=5.0$ μm (closed circles and open square markers, respectively), trapped in an optical lattice of period L (solid curves represent the intensity distribution): (a) $L=0.8D_2$, (b) $L=0.625D_2$. All curves are normalized respect to the maximum value of the force for the 5.0 μm particle with $L=0.8D_2$. Bottom row: transverse intensity distributions showing the equilibrium positions of the particles.

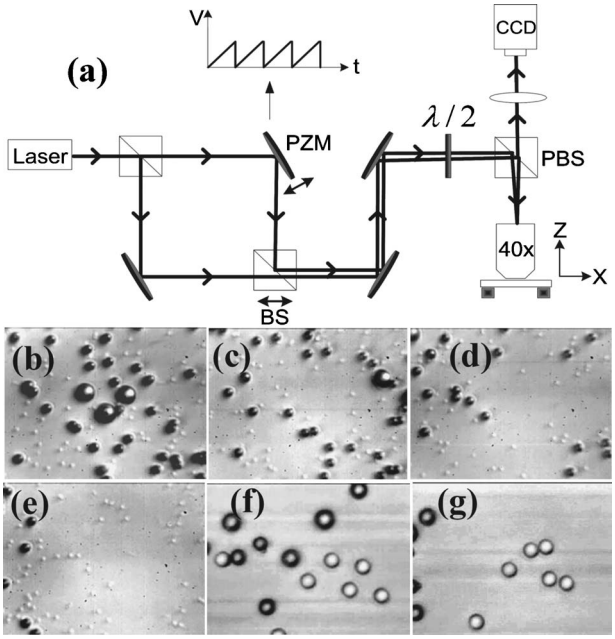

FIG. 2. (a) Experimental setup. The mirror mounted on a piezoelectric (PZM) is driven with a sawtooth time modulation function to generate a vibrating interference pattern; the period of the fringes is set by displacing the beamsplitter BS. Frames (b)–(e) show sorting of three types of particles: 1 μm diameter silica particles and 2 and 5 μm latex particles. (b) All particles are mixed together; (c) the 5 μm particles are removed to the right; (d)–(e) 2 μm particles are removed in the opposite direction (EPAPS E-APPL AB-88-01960). Frames (f)–(g) show sorting of 5 μm diameter spheres of latex and silica (latex looks darker than silica) (REFERENCE EPAPS Sorting5-5microns.avi).

function of the position x_0 of the particle within the beam profile and the corresponding equilibrium positions, for the case of a stationary interference pattern for two latex spheres ($n=1.59$) with diameters $D_1=2.0$ μm and $D_2=5.0$ μm (closed circles and open square markers, respectively). Columns correspond to spatial periods of (a) $L=0.8D_2$, (b) $L=0.625D_2$, while the top and bottom rows correspond to optical forces and intensity distributions showing the equilibrium positions of the particles, respectively. Only small regions of the pattern are shown and the intensity profile (solid line) is also plotted as a reference. Stable equilibrium positions where the particles can be trapped are associated to the points where the force is zero and the curve has positive slope, since any displacement of the sphere would give rise to a restoring force in the opposite direction. In the case of column (a), both particles are trapped at the intensity maxima and the magnitude of the force is stronger for the larger sphere. From Eq. (1) it is seen that the optical force is proportional to the square of the particle's radius. However, in the case of a periodical landscape of light, where bright and dark regions alternate, the force strongly depends on the particle's size relative to the spatial period of the fringes. For instance, there is a threshold value, corresponding approximately to $L/D\cong 0.63$, for which the trapping positions shift from the intensity maxima to the intensity *minima*, and the magnitude of the optical force falls rapidly. This behavior is illustrated in column (b), where the force is now stronger for the *smaller* sphere. In this case, the smaller spheres will be locked-in to the moving pattern whereas larger spheres will respond less to it.

On the other hand, for particles of the same size with different refractive index, the curves for the optical force are very similar in shape but scaled, since the magnitude of the force depends on the relative refractive index of the particle respect to the medium via the reflectance and transmittance coefficients, being smaller for particles with lower refractive index.[10] In practice, the separation of equally sized particles of different materials can be accomplished by gradually increasing the power until reaching the minimum power level required for moving only the particles with higher refractive index. This method, however, becomes less efficient as the size of the particles increases, since the power threshold is lower for larger particles, giving rise to a very slow separation rate.

In the experiment we introduced the beam of an argon ion laser ($\lambda=488$ nm) into a Mach-Zehnder interferometer, as shown in Fig. 2(a). The output pattern of fringes is directed towards a 40× microscope objective. The spatial period of the fringes can be tuned easily from 0.7 up to 27 μm by shifting the beam splitter (BS) along the x direction. The power at the sample cell is controlled by means of the $\lambda/2$ wave plate and the polarizing beamsplitter (PBS). The mirror PZM is mounted on a piezoelectric driven by an arbitrary function generator. The use of an asymmetric driving function, like the sawtooth function represented by $\phi(t)$ in Eq. (2), results in a sweeping-like movement of the fringes allowing the optical sorting. The optimum value for ϕ_0 was found to be 2π, which warranties a constant forward movement of the particles, since they will be always placed in a stable equilibrium position. Sign inversion of sawtooth function's slope reverses the transport current of the particles.

Fractionation capabilities of our technique are demonstrated in Figs. 2(b)–2(e), where the sequence of frames shows the separation of three kinds of particles (1 μm diameter particles of silica and 2 and 5 μm particles of latex) mixed in distilled water E-APPLAB-88-019610.[12] Frame (b) shows the initial mixture. Frame (c) shows the separation process for the 5 μm particles, which are moved to the right by setting $L=10$ μm and a power level of 150 mW. In

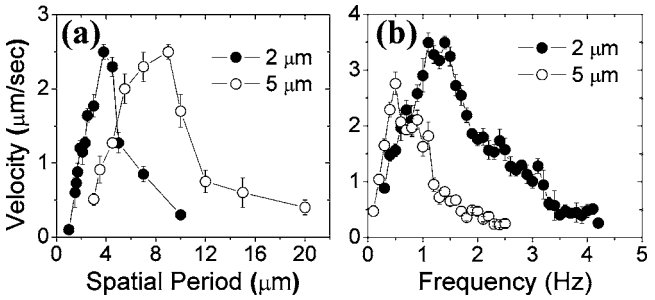

FIG. 3. (a) Experimental curves for the velocity of the particles as a function of the spatial period of the fringes for latex spheres of 2 and 5 μm diameter (fixed power $P=130$ mW and frequency $f=1$ Hz). (b) Velocity as a function of the PZM vibration frequency for the same particles (optimum period for each particle and fixed power $P=130$ mW).

frames (d)–(e), the 2 μm particles are moved in the opposite direction by reversing the sign of the slope of the sawtooth function and changing the period of the interference fringes to $L=4$ μm. In principle, more than three types of particles may be separated from the initial mixture by sending them towards different directions by rotating the orientation of the fringes.

On the other hand, Fig. 2, frames (f)–(g) show sorting of particles of the same size (5 μm diameter) of latex ($n=1.59$) and silica ($n=1.45$) (Reference EPAPS Sorting5-5microns.avi). In the figure, latex particles, which look darker than silica particles, are moved to the left. If the threshold power for start moving the latex spheres ($\sim$100 mW) is increased by only 10%, then both kinds of particles are locked-in to the pattern and sorting cannot occur.

The performance of the system can be further evaluated by means of Fig. 3, where the experimental plots show the variation of the average transport velocity for 2 and 5 μm diameter particles as a function of (a) the spatial period of the fringes ($P=130$ mW and $f=1$ Hz) and (b) the vibration frequency ($P=130$ mW and period optimized for each particle size). The maximum velocity ($v_{\max}\approx 2.5$ μm/s) is reached when the spatial period is about $L\cong 1.75D$ for both types of particles. On the other hand, Fig. 3(b) shows an optimum value for the frequency of 1.2 and 0.5 Hz for 2 and 5 μm particles, respectively. For small vibration frequencies, it is expected that the velocity of the dragged particles increases with frequency. However, if the pattern of fringes moves too fast, the particles will not be able to follow it anymore, since they will sense a time-averaged optical force rather than a moving light pattern, as seen in scanning-beam multiple traps.[13,14] According to our experimental results, the transition between the two situations mentioned earlier is not abrupt, but the velocity of a particle gradually decreases after reaching an optimum value for the vibration frequency, which is inversely proportional to the particle's mass. The maximum velocity we obtained $v_{\max}$ can be increased by increasing the beam power. For the maximum power reaching the sample, $P=200$ mW, we obtained $v_{\max}\approx 6.5$ μm/s.

We have demonstrated a new technique for optical sorting of polydisperse mixtures that may contain more than two kinds of particles, which does not involve microfluidic flow. We notice that this method could be used to analyze unknown polydisperse mixtures with a proper calibration process by determining optimum control parameters (period of the fringes, vibration frequency and incident power).

The authors are very grateful to Professor Kishan Dholakia for his valuable comments and suggestions. K.V.-S. acknowledges support of DGAPA-UNAM-IN103103.

[1] A. Ashkin, Phys. Rev. Lett. **24**, 156 (1970).
[2] H. A. Pohl, *Dielectrophoresis* (Cambridge University Press, Cambridge, 1978.
[3] P. Y. Chiou, A. T. Ohta, and M. C. Wu, Nature (London) **436**, 370 (2005).
[4] T. Imasaka, Y. Kawabata, T. Kaneta, and Y. Ishidzu, Anal. Chem. **67**, 1763 (1995).
[5] M. P. MacDonald, G. C. Spalding, and K. Dholakia, Nature (London) **426**, 421 (2003).
[6] K. Ladavac, K. Kasza, and D. G. Grier, Phys. Rev. E **70**, 010901 (2004).
[7] J. Glückstad, Nat. Mater. **3**, 9 (2004).
[8] P. Zemánek, V. Karesek, and A. Sasso, Opt. Commun. **240**, 401 (2004).
[9] A. N. Rubinov, J. Phys. D **36**, 2317 (2003).
[10] K. Volke-Sepúlveda, S. Chávez-Cerda, V. Garcés-Chávez, and K. Dholakia, J. Opt. Soc. Am. B **21**, 1749 (2004).
[11] R. Gussgard, T. Lindmo, and I. Brevik, J. Opt. Soc. Am. B **9**, 1922 (1992).
[12] See EPAPS Document No. E-APPLAB-88-019610 for two multimedia files (AVI) of optical sorting. A direct link to this document may be found in the online article's HTML reference section. The document may also be reached via the EPAPS homepage (http://www.aip.org/pubservs/epaps.html) or from ftp.aip.org in the directory/epaps. See the EPAPS homepage for more information.
[13] K. Sasaki, M. Koshioka, H. Misawa, N. Kitamura, and H. Masuhara, Opt. Lett. **16**, 1463 (1991).
[14] C. Mio, T. Gong, A. Terray, and D. M. Marr, Rev. Sci. Instrum. **71**, 2196 (2000).